

Recruitment dynamics in adaptive social networks

Maxim S. Shkarayev,¹ Ira B. Schwartz,² and Leah B. Shaw¹

¹*Applied Science Department, College of William & Mary, Williamsburg, VA 23187*

²*Nonlinear Systems Dynamics Section, Plasma Physics Division,
Code 6792, US Naval Research Laboratory, Washington, DC 20375*

(Dated: October 28, 2018)

We model recruitment in adaptive social networks in the presence of birth and death processes. Recruitment is characterized by nodes changing their status to that of the recruiting class as a result of contact with recruiting nodes. Only a susceptible subset of nodes can be recruited. The recruiting individuals may adapt their connections in order to improve recruitment capabilities, thus changing the network structure adaptively. We derive a mean field theory to predict the dependence of the growth threshold of the recruiting class on the adaptation parameter. Furthermore, we investigate the effect of adaptation on the recruitment dynamics, as well as on network topology. The theoretical predictions are compared with direct simulations of the full system. We identify two parameter regimes with qualitatively different bifurcation diagrams depending on whether nodes become susceptible frequently (multiple times in their lifetime) or rarely (much less than once per lifetime).

Keywords: adaptive networks, network dynamics, recruitment

I. INTRODUCTION

Any society contains individuals who may belong to a religion or political party and in general are carriers of an ideology or fad that they desire to spread to the rest of the society. Thus, for a given ideology, a society can be partitioned into a set of people that represent the ideology and want to spread it, and the complement of this set. For example, ideology could correspond to the views of a particular political party, with the party members desiring to recruit new members to improve their positions in the government. Some work in this direction is presented in the papers studying voter models in which individuals make connections to influence others' opinions [1–3], as well as opinion dynamics models in which individuals are influenced by neighbors' opinions [4]. Other areas of recruitment have been proposed as mechanisms for fads which appear as a rapid rise above some threshold, as in music [5], management technologies [6], economics [7], and even science [8]. Slower recruitment based on social networks has been postulated in biology [9] and the spread of alcoholism [10]. Slowing the rise of a fad or eliminating the spread of an ideology has been also been proposed through the control of critical nodes in a social network [11].

A direction that is particularly important today is collisions between ideologies that can lead to radicalization of society. Recently, mathematical modeling of various radical ideas, such as terrorist organizations and their dynamics, has been done to explore their structure and organization [12–14]. A

number of recent publications discuss terrorist networks as optimal structures that optimize communication efficiency, while balancing the secrecy of the networks [18–20]. In addition to the dynamical approaches that measure rates of attacks of radical groups [15], operations research theories have been applied to the formation of radical groups [16]. Models exist for terrorist recruitment as a spreading process within a well-mixed population [21, 23] or a social network [21–23]. In [17], a systematic analysis of recruitment to Hezbollah was done. It uses models from dynamical systems based on data from a political science discipline to generate a compartmental model of recruitment. Although the modeling is deterministic, it considers various parameters that explicitly affect the success of recruitment to the radical cause. However, all of these models for dynamics of recruitment consider populations that are well-mixed or that have a fixed social network structure. Changes in the network structure to promote recruiting are not included.

We develop a simple model of a society in which some of the members belong to a class that tries to spread an ideology. The ideology spreads as a result of contact of recruiting members with non-recruiting members. The recruiting members may improve their chances to recruit via network adaptation. The purpose of the adaptation proposed here is to improve the spread of the ideology, which is in contrast to adaptation in the epidemiological models [24, 25] where the purpose is avoidance of contact with the spreading members. In addition to adaptation, the connectivity within the society changes

due to birth of new members and death of existing members. Using this model we explore how the existence of stable recruiting classes depends on the adaptation and other parameters. We also consider the network topology of the recruiting class, as it may be important in accessing the quality of the communication channels in the resulting structure. Section II presents the model and a system of mean field equations describing its dynamics. Section III presents mean field analysis of the threshold for successful recruiting and its dependence on the network adaptation, compares these results with simulations of the full system, and considers the network geometry of the recruiting class. Section IV concludes.

II. MODELING THE DYNAMICS OF RECRUITMENT

A. The Model

We consider a social structure consisting of M individuals represented by nodes in a network. An existing relation between any two individuals is represented by a link between the two nodes. New individuals join the society at a constant total rate μ , and the individuals in the network can leave the network via death at rate δ per individual. When new individuals join the system, they arrive with σ links, which are connected to σ randomly selected nodes in the population. When individuals die, their links are removed.

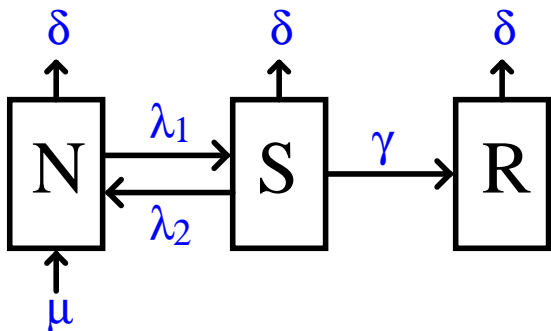


FIG. 1. Schematic representation of node fluxes in and out of the network due to birth and death, described by the rates μ and δ respectively. Fluxes between the three classes are described by the transition rates λ_1 , λ_2 and γ . Link rewiring (not shown here) takes place at rate w .

Some members of the society, *recruiters* (also referred to as R-nodes), are carriers of an ideology that they try to spread to the individuals they come

into contact with. The individuals that do not belong to the recruiting class are divided into two groups: those who are *susceptible* to the recruitment (S-nodes) and those who are *non-susceptible* (N-nodes). We assume that individuals can spontaneously change their state from non-susceptible to susceptible and vice versa (with rates λ_1 and λ_2 respectively). An individual in the recruiting class remains in that class until death [21].

A susceptible individual joins the recruiting class at a rate that is proportional (with proportionality constant γ) to the number of contacts it has with the recruiting class. In order to improve their recruiting capabilities, the recruiting individuals can rewire their links, abandoning a connection to the nonsusceptible individuals in favor of connection to a susceptible node. As the links are rewired, the network topology changes based on the current states of its nodes. The schematic representation of the node dynamics is shown on Fig. II A.

We perform Monte Carlo simulations of the above system following the continuous time algorithm described in [26]. We start with an Erdos-Renyi random network, which then evolves according to the rules of birth, death, and rewiring. The results presented in the rest of the paper are for the systems that have reached a steady state.

B. Mean field

To describe the dynamics of this system, we construct a mean field model for nodes and links as in [24]. The time evolution of the nodes of each type is described by the following rate equations:

$$\partial_t \mathcal{N}_N = \mu - \lambda_1 \mathcal{N}_N + \lambda_2 \mathcal{N}_S - \delta \mathcal{N}_N \quad (1a)$$

$$\partial_t \mathcal{N}_S = \lambda_1 \mathcal{N}_N - \lambda_2 \mathcal{N}_S - \gamma \mathcal{N}_{RS} - \delta \mathcal{N}_S \quad (1b)$$

$$\partial_t \mathcal{N}_R = \gamma \mathcal{N}_{RS} - \delta \mathcal{N}_R, \quad (1c)$$

Here the functions $\mathcal{N}_N \equiv \mathcal{N}_N(t)$, $\mathcal{N}_S \equiv \mathcal{N}_S(t)$, $\mathcal{N}_R \equiv \mathcal{N}_R(t)$ represent the number of nodes of each type. The process of recruitment is captured by the $\gamma \mathcal{N}_{RS}$ term, where the recruitment is shown to take place at a rate proportional to the number of links between the recruiting class and the susceptible class, \mathcal{N}_{RS} .

In order to capture the rewiring process, we follow the evolution of the number of different types of links

present in the network:

$$\begin{aligned} \partial_t \mathcal{N}_{\text{NN}} &= \lambda_2 \mathcal{N}_{\text{SN}} + \sigma \mu \frac{\mathcal{N}_{\text{N}}}{\mathcal{N}_{\text{N}} + \mathcal{N}_{\text{S}} + \mathcal{N}_{\text{R}}} \\ &\quad - 2(\lambda_1 + \delta) \mathcal{N}_{\text{NN}} \end{aligned} \quad (2a)$$

$$\begin{aligned} \partial_t \mathcal{N}_{\text{SN}} &= \sigma \mu \frac{\mathcal{N}_{\text{S}}}{\mathcal{N}_{\text{N}} + \mathcal{N}_{\text{S}} + \mathcal{N}_{\text{R}}} - \gamma \mathcal{N}_{\text{NSR}} + 2\lambda_2 \mathcal{N}_{\text{SS}} \\ &\quad - (\lambda_1 + \lambda_2 + 2\delta) \mathcal{N}_{\text{SN}} + 2\lambda_1 \mathcal{N}_{\text{NN}} \end{aligned} \quad (2b)$$

$$\begin{aligned} \partial_t \mathcal{N}_{\text{SS}} &= -\gamma \mathcal{N}_{\text{SSR}} + \lambda_1 \mathcal{N}_{\text{SN}} \\ &\quad - 2(\lambda_2 + \delta) \mathcal{N}_{\text{SS}} \end{aligned} \quad (2c)$$

$$\begin{aligned} \partial_t \mathcal{N}_{\text{RN}} &= \gamma \mathcal{N}_{\text{NSR}} + \sigma \mu \frac{\mathcal{N}_{\text{R}}}{\mathcal{N}_{\text{N}} + \mathcal{N}_{\text{S}} + \mathcal{N}_{\text{R}}} \\ &\quad - (\lambda_1 + 2\delta + w) \mathcal{N}_{\text{RN}} + \lambda_2 \mathcal{N}_{\text{RS}} \end{aligned} \quad (2d)$$

$$\begin{aligned} \partial_t \mathcal{N}_{\text{RS}} &= -\gamma \mathcal{N}_{\text{RSR}} + \gamma \mathcal{N}_{\text{SSR}} \\ &\quad - (\lambda_2 + 2\delta) \mathcal{N}_{\text{RS}} + (\lambda_1 + w) \mathcal{N}_{\text{RN}} \end{aligned} \quad (2e)$$

$$\partial_t \mathcal{N}_{\text{RR}} = \gamma \mathcal{N}_{\text{RSR}} - 2\delta \mathcal{N}_{\text{RR}}. \quad (2f)$$

where the terms \mathcal{N}_{xy} correspond to the number of links connecting nodes from classes x and y , e.g., \mathcal{N}_{NN} corresponds to the number of NN links. The terms proportional to $\sigma\mu$ correspond to the influx of edges due to the birth of new nodes, where the probability for the new node to attach itself to a node from class X is proportional to the number of nodes in that class. The third order terms, \mathcal{N}_{NSR} , \mathcal{N}_{SSR} and \mathcal{N}_{RSR} , describe the formation of triples of nodes with an S-node at the center, and at least one of the edges terminating at an R-node. These terms describe the rate at which NS-, SS- and RS-links become NR-, SR- and RR- links respectively, due to the interaction of the central S-node with its neighboring R-node. Note that our definition of RSR triples includes *degenerate* triples, i.e., RSR triples where both of the R-node ends correspond to the same R-node, by analogy with degenerate triangles.

The resulting system of equations is not closed, as it contains higher order terms. Following earlier works in epidemiology [27], we introduce the closure based on the assumption of a homogeneous distribution of RS-links:

$$\mathcal{N}_{\text{NSR}} = \frac{\mathcal{N}_{\text{SN}} \mathcal{N}_{\text{RS}}}{\mathcal{N}_{\text{S}}} \quad (3a)$$

$$\mathcal{N}_{\text{SSR}} = 2 \frac{\mathcal{N}_{\text{RS}} \mathcal{N}_{\text{SS}}}{\mathcal{N}_{\text{S}}} \quad (3b)$$

$$\mathcal{N}_{\text{RSR}} = \frac{\mathcal{N}_{\text{RS}}^2}{\mathcal{N}_{\text{S}}} + \mathcal{N}_{\text{RS}}. \quad (3c)$$

We thus obtain a system of nine mean field equations, which we analyze.

III. RESULTS

A. Mean field recruiting threshold

We first consider the bifurcation point of the recruitment model where the zero recruit (trivial) steady state becomes unstable. This is a transcritical bifurcation point, which is analogous to the epidemic onset in epidemic spreading models. It can be found analytically as a function of parameters for the mean field model, and certain asymptotic limits have a simple form.

We nondimensionalize Eqns. (1) and (2) to simplify the analysis. We introduce the dimensionless time variable $\tilde{t} \equiv \delta t$, where time is rescaled by the average node lifetime δ^{-1} . Further, the node variables are rescaled by the expected population size at steady state, μ/δ , while the link variables are rescaled by the expected number of links at steady state, $(\mu/\delta)(\sigma/2)$. Let $\mathbf{x} \equiv [\mathcal{N}_{\text{N}}, \mathcal{N}_{\text{S}}, \mathcal{N}_{\text{R}}, \mathcal{N}_{\text{NN}} 2\sigma^{-1}, \mathcal{N}_{\text{SN}} 2\sigma^{-1}, \mathcal{N}_{\text{SS}} 2\sigma^{-1}, \mathcal{N}_{\text{RN}} 2\sigma^{-1}, \mathcal{N}_{\text{RS}} 2\sigma^{-1}, \mathcal{N}_{\text{RR}} 2\sigma^{-1}] \delta \mu^{-1}$ denote the 9-dimensional vector of rescaled node and link state variables. Note that in the steady state the rescaled node variables sum to 1, and, therefore, in steady state they correspond to the probability for a node of a given type to exist in the system. Similarly, the rescaled link variables sum to 1, and correspond to the probability for an edge chosen at random to be of a given type, e.g., at steady state x_8 corresponds to the probability for a randomly chosen edge to be an RS link.

We introduce the following rescaled parameters:

$$\Lambda_1 \equiv \lambda_1 \delta^{-1} \quad (4a)$$

$$\Lambda_2 \equiv \lambda_2 \delta^{-1} \quad (4b)$$

$$\Gamma \equiv (\gamma \sigma / 2) \delta^{-1} \quad (4c)$$

$$W \equiv w \delta^{-1} \quad (4d)$$

We can now write the dimensionless equations of motion as

$$\dot{\mathbf{x}} = \mathbf{F}(\mathbf{x}; \bar{\Lambda}). \quad (5)$$

where $\bar{\Lambda} \equiv [\Lambda_1, \Lambda_2, W, \Gamma, \sigma]$ is a vector of all the system parameters. (Recall that σ is a dimensionless integer.) The full system of dimensionless equations is given in Eqns. (A1).

We can now find the trivial steady state solution, where the number of R nodes is zero. This restricts the state to be of the form $\mathbf{x}_0 = [x_{0,1}, x_{0,2}, 0, x_{0,4}, x_{0,5}, x_{0,6}, 0, 0, 0]$, where the number of links involving R nodes is zero as well. This

guarantees that $F_i(\mathbf{x}_0, \bar{\Lambda}) = 0$ for $i = 3, 7, 8, 9$. Since this subset of equations represents an invariant manifold, we concentrate on solving the equations for the rest of the 5 components, $x_{0,1}$, $x_{0,2}$, $x_{0,4}$, $x_{0,5}$ and $x_{0,6}$.

The first observation is that the x_1 and x_2 equations are solvable when the number of recruiting nodes is zero, and they yield steady state values of

$$x_{0,1} = (\Lambda_2 + 1)D^{-1}, \quad (6a)$$

$$x_{0,2} = \Lambda_1 D^{-1}, \quad (6b)$$

where $D \equiv \Lambda_1 + \Lambda_2 + 1$. The non-zero link equations may be expressed in terms of $x_{0,1}$, $x_{0,2}$, and they are given by the following:

$$x_{0,4} = (\Lambda_2 + 1)^2 D^{-2}, \quad (6c)$$

$$x_{0,5} = 2\Lambda_1(\Lambda_2 + 1)D^{-2}, \quad (6d)$$

$$x_{0,6} = \Lambda_1^2 D^{-2}. \quad (6e)$$

Now that we have the full trivial solution, we can examine its stability. In order to do this, we linearize the vector field about \mathbf{x}_0 , and examine where it has a one dimensional null space. That is, at the bifurcation point, there is only one real eigenvalue passing through zero. This is equivalent to examining where the determinant of the Jacobian vanishes; i.e., we compute those parameters where

$$\det(\mathcal{D}_{\mathbf{x}}\mathbf{F}(\mathbf{x}_0, \bar{\Lambda})) = 0. \quad (7)$$

The following relation describes the location of the bifurcation:

$$W = -\Lambda_1 \left[1 + \frac{2\Gamma}{[\Gamma(2 - \sigma^{-1}) - 1](\Lambda_1 + \Lambda_2 + 1)} \right] + \Lambda_2 \frac{1}{\Gamma(2 - \sigma^{-1}) - 1} + \frac{2(\Gamma\sigma^{-1} + 1)}{\Gamma(2 - \sigma^{-1}) - 1} \quad (8)$$

We next examine the limits of Eq. (8) when either the recruitment rate Γ or rewiring rate W is large. The minimum amount of recruitment required to maintain nonzero values of recruited population, when W approaches infinity, can be found by setting the least common denominator of Eq. (8) to zero, which yields a simple expression for Γ :

$$\Gamma = \frac{1}{2 - \sigma^{-1}} \quad (9)$$

If the recruitment rate is below this value, additional rewiring is not sufficient to enable spreading of the recruiting class.

Similarly, we find the smallest amount of rewiring required for existence of a nontrivial steady state solution, conditioned on our ability to control Γ , with all the other parameters fixed:

$$\lim_{\Gamma \rightarrow \infty} W = -\Lambda_1 \left[1 + \frac{2}{(2 - \sigma^{-1})(\Lambda_1 + \Lambda_2 + 1)} \right] + 2 \frac{\sigma^{-1}}{2 - \sigma^{-1}}$$

For lower rewiring rates, the recruiting class cannot spread even if the recruiting rate is large. The value of this asymptote is greatest, meaning rewiring is most necessary, when Λ_1 approaches zero. In this case few non-susceptible nodes become susceptible to recruiting, and the necessary rewiring value approaches

$$W = \frac{2\sigma^{-1}}{2 - \sigma^{-1}} \quad (10)$$

B. Comparison of mean field with simulations

We next compare the mean field predictions for the spread of recruiters with simulations of the full stochastic network system. Thus, we compare the average size of recruited portion of population in statistical steady state, to the solution of the mean-field equations at steady state, which we solve exactly in the Appendix A. We assume that the parameters Λ_1 and Λ_2 (rates for gaining and losing susceptibility) and σ (determines average degree) depend on details of the society. On the other hand, we assume that the parameters Γ and W can be controlled by the recruiters, i.e., the recruiters may choose to be more or less aggressive in their recruitment, as well as in how quickly they rewire their links to susceptible members of society. Therefore, we investigate the recruiting effectiveness for a given choice of Λ_1 , Λ_2 and σ , while varying Γ and W .

We distinguish two parameter regimes, corresponding to two qualitatively different behaviors of the system: small values of Λ_1 ($\Lambda_1 \ll 1$) and large values of Λ_1 ($\Lambda_1 \gg 1$). The small Λ_1 regime corresponds to the case where nodes become susceptible to recruiting only rarely, on average much less than once in their lifetime. The large Λ_1 regime corresponds to the case where, on average, nodes become susceptible to recruiting at least once in their lifetime.

In Figs. 2 and 3 we show the results of simulating the system in these two regimes. The density

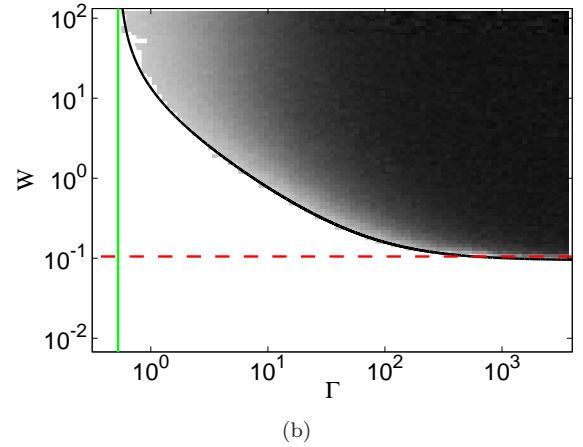
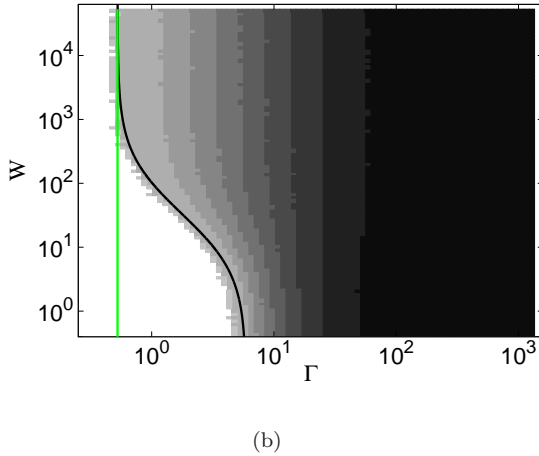
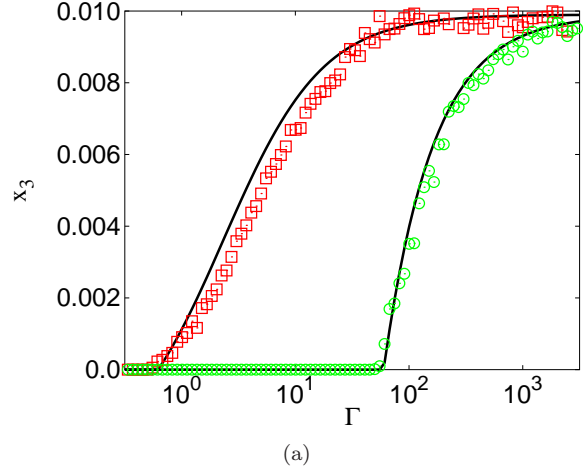
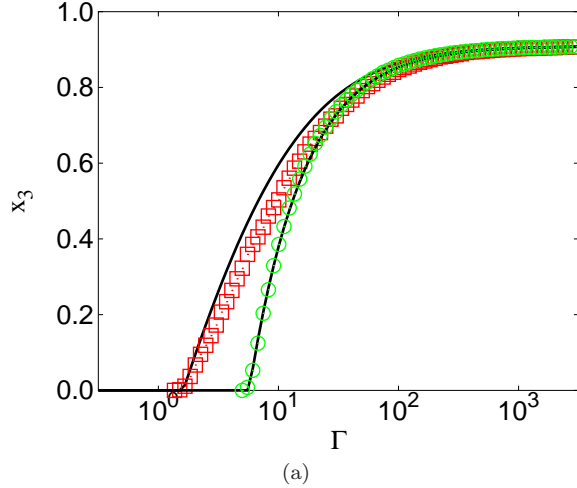


FIG. 2. Direct numerical simulation of a stochastic network system with $\lambda_1 \gg 1$. In Fig. 2(a) we compare the result of the simulation (symbols) to the mean field solution given by Eq. (A18) (solid curves). Square (red online): strong rewiring, $W \approx 40$. Circle (green online): weak rewiring, $W \approx 0.4$. Fig. 2(b) shows the density plot representing the dependence of the fraction of recruited nodes in the population in statistical steady state on rescaled rates of rewiring, W , and recruiting, Γ . Vertical solid line (green online) corresponds to the minimum recruitment rate required to support a nontrivial solution, as given by Eq. (9). The dashed curve corresponds to the recruiting threshold as predicted by mean field in Eq. (10). The simulations are performed on a system with $\mu = 10^5$, $\delta = 1$, $\sigma = 10$, $\lambda_1 = 10$, $\lambda_2 = 100$. The time averaged values are computed once the system reaches steady state regimes (in all of the figures in this paper this corresponded to at least $10\delta^{-1}$ units of time, in other words about 10 generations of nodes have died before we assume the system to be at the steady state)

FIG. 3. In Fig. 3(a) we compare the result of the simulation to the mean-field solution given by Eq. (A18). Square (red online): strong rewiring, $W \approx 70$. Circle (green online): weak rewiring, $W \approx 0.2$. Fig. 3(b) shows the density plot representing the dependence of the fraction of recruited nodes in the population in statistical steady state on rescaled rates of rewiring, W , and recruiting, Γ . Vertical solid line (green online) correspond to the minimum recruitment rate required to support nontrivial solution, as given by Eq. (9). Horizontal solid line (red online) corresponds to the rewiring rate that guarantees existence of nontrivial solution in the limit of large recruitment rate (Note this asymptote is approached in the limit of small λ_1 .) The dashed curves correspond to the recruiting threshold as predicted by mean field in Eq. (10). The simulations are performed on a system with $\mu = 10^5$, $\delta = 1$, $\sigma = 10$, $\lambda_1 = 0.01$, $\lambda_2 = 10$.

plots in Figs. 2(b) and 3(b) show the fraction of recruited nodes as a function of recruiting rate Γ and rewiring rate W in the networks with $\lambda_1 \gg 1$

and $\Lambda_1 \ll 1$ respectively. The black curves in the two figures represent the location of the recruiting threshold as derived from the mean field equations and are given by Eq. (8). Here mean field allows us to accurately predict the onset of the stable nontrivial solution. In Figs. 2(a) and 3(a) we compare the simulation results to the mean field predictions. Even though there is some discrepancy between the direct simulations and the mean field near the bifurcation, the recruiting threshold and the asymptotic behavior for large Γ show excellent agreement with the simulations.

For the parameter values we have studied, the trivial steady state solution undergoes a forward transcritical bifurcation for all values of W where nontrivial solution exists. This is in contrast with backward transcritical bifurcations and bistability observed in epidemiological models where the purpose of the rewiring is avoidance of the nodes spreading infection [24, 28, 29]. Note that, unlike those models, the purpose of the rewiring in the recruitment model is attraction of the susceptible population by the recruiters.

We would like to draw the reader's attention to an important difference in the system behavior in the two regimes. In the regime where $\Lambda_1 \gg 1$ the nontrivial solution exists for all values of W as long as Γ is sufficiently large. On the other hand, in the regime where $\Lambda_1 \ll 1$ the nontrivial solution may fail to exist for any value of Γ unless rewiring is aggressive enough. In Fig. 3(b) there is a range of rewiring rates W for which only trivial solutions exist. The horizontal dashed line, given by Eq. (10), indicates the level of rewiring that is sufficient for the nontrivial solution to exist at rapid recruiting (large Γ). This example demonstrates that the minimum rewiring rate for the nontrivial solution to exist approaches the predicted level in Eq. (10) for small values of Λ_1 .

Another important difference between the two regimes of Λ_1 values is seen when we compare two systems with different values of Λ_1 and Λ_2 while the ratio $\Lambda_1/(1 + \Lambda_2)$ is kept fixed. Note that in the absence of recruitment, such systems have identical sizes of nonsusceptible and susceptible classes. In other words, in the presence of recruitment, the pool of individuals available for recruitment would appear to be the same. However, as we can see from Fig. 4, there is a significant difference in the size of recruited population as well as the recruiting threshold. The difference appears to be caused by the difference in the dynamics in the two regimes. Thus, for the large values of Λ_1 and Λ_2 a node can become susceptible several times during its life, while, as the value of

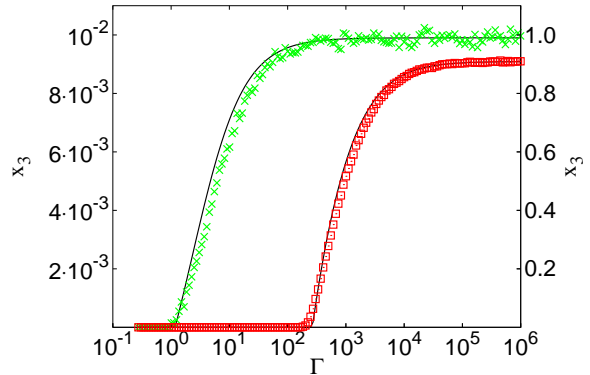


FIG. 4. Comparing systems with different values of Λ_1 , but same ratio of $\Lambda_1/(1 + \Lambda_2)$. Squares (red online), right axis: $\Lambda_1 = 10$, $\Lambda_2 = 10^4$. Crosses (green online), left axis: $\Lambda_1 = 0.01$, $\Lambda_2 = 9.001$. Both of the simulations were performed with the following parameters: $w = 10$, $\mu = 10^5$, $\delta = 1$, $\sigma = 10$.

Λ_1 decreases, only some nodes will ever become susceptible, with low likelihood of doing so more than once.

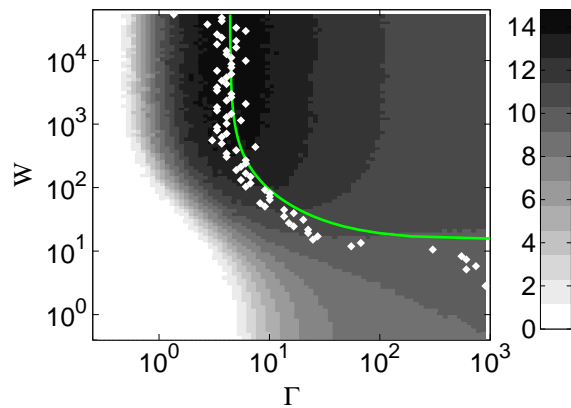


FIG. 5. Direct numerical simulation. Density plot representing the dependence of the fraction of the mean node degree in R-subnetwork in steady state, $2N_{RR}/N_R$, on rescaled rates of rewiring, W , and recruiting, Γ . Solid line (green online) indicates the value of Γ where the degree is at a maximum for a given value of W , found using analytic expression in Eq. (B4). The white diamonds correspond to the location of the maximum in simulations for a given value of W . The simulations are performed with the following parameters: $\mu = 10^5$, $\delta = 1$, $\sigma = 10$, $\lambda_1 = 10$, $\lambda_2 = 100$.

C. Recruited subnetwork geometry

We now investigate the structure of the portion of the network (later referred to as the R-subnetwork) consisting only of R-nodes and links between them. In particular, we are interested in the mean degree of its nodes when the system reaches a steady state. The mean field approach, in addition to predicting the fraction of recruited nodes (which corresponds to the size of the R-subnetwork), also provides information about topology of the subnetwork in the form of mean degree of the nodes. The mean degree of a node in the subnetwork serves as a low order description of how well the nodes in the network are connected, which may be important for communication within the established subnetwork. The density plot in Fig. 5 shows the dependence of the mean degree on W and Γ . The nonmonotonic behavior as a function of Γ for fixed W is predicted by the mean field model. The solid line corresponds to the analytical prediction of the maximum's location as given by Eq. (B4) derived in Appendix B. Note that the analytic description of the maximum's location would allow the recruiting class to optimize connectivity within the subnetwork, if that happens to be an important parameter for that class. The mean-field approximation fails to capture the nonmonotonic behavior of the mean-degree in the limit where $\Lambda_1 \ll 1$, and we leave this issue to our next paper.

IV. CONCLUSIONS AND DISCUSSION

We develop a simple model that describes a process of recruitment of new members by a recruiting class within a society. The members of the recruiting class can improve their recruiting capabilities via network adaptation. Thus, they may choose to abandon their relations with those members of society that are not prone to the particular recruitment. This model assumes that once a node joins the recruiting class, it becomes a recruiter and remains a member of this class until death.

We have develop and analyzed a mean-field model of the system. Thus, we are able to accurately predict the onset of the stable nontrivial solution of the system at steady state. Furthermore, we are able to accurately predict the size of the recruited class for a given set of system parameters, as well as the mean degree of the subnetwork formed by the recruited members. We compare the predictions made by the mean-field description with the direct simulations of

our model. We observe a good agreement between the model and its mean-field approximation.

Analyzing the mean-field model, we find two parameter regimes with very distinct qualitative behavior. Thus, we show that in the society where a particular ideology (perhaps corresponding to radical ideology) is unpopular and few members are susceptible to it, adaptation is necessary in order to observe stable nonzero levels of the recruiting class. On the other hand, if the idea is sufficiently popular that individuals frequently become susceptible (eg., recruitment into a political party), the adaptation improves the recruiting capabilities and may affect the ultimate topology of the recruited, but adaptation may not be a necessary condition for the existence of nonzero stable solution. Furthermore, we speculate that if our model were be extended to a society with two competing recruiting classes (as in a two party system), the adaptation may be a mechanism by which one competing class gets an edge over the other class.

As evidenced by the results presented in Figs. 2(a) and 3(a), the mean-field approximation has some shortcomings when it comes to an accurate description of the system in the parameter regime between the bifurcation point and the asymptotic saturation. As a future extension, we will develop and analyze a new closure of the mean-field equations to improve the accuracy.

ACKNOWLEDGMENTS

MSS and LBS were supported by the Army Research Office, Air Force Office of Scientific Research, and by Award Number R01GM090204 from the National Institute Of General Medical Sciences. The content is solely the responsibility of the authors and does not necessarily represent the official views of the National Institute Of General Medical Sciences or the National Institutes of Health. IBS was supported by the Office of Naval Research and the Air Force Office of Scientific Research.

Appendix A: Exact solution

In this appendix, we derive the exact solution to the system of equations in Eqs. (1) and (2) when the system is at the nontrivial steady state, i.e., when the left hand side of the equations is zero. We begin by deriving the dimensionless equations, as proposed

in section III A:

$$\partial_t x_1 = 1 - \Lambda_1 x_1 + \Lambda_2 x_2 - x_1 \quad (\text{A1a})$$

$$\partial_t x_2 = \Lambda_1 x_1 - \Lambda_2 x_2 - \Gamma x_8 - x_2 \quad (\text{A1b})$$

$$\partial_t x_3 = \Gamma x_8 - x_3 \quad (\text{A1c})$$

$$\partial_t x_4 = \Lambda_2 x_5 + 2 \frac{x_1}{x_1 + x_2 + x_3} - 2(\Lambda_1 + 1)x_4 \quad (\text{A1d})$$

$$\partial_t x_5 = 2 \frac{x_2}{x_1 + x_2 + x_3} - \Gamma \frac{x_5 x_8}{x_2} + 2\Lambda_2 x_6 - (\Lambda_1 + \Lambda_2 + 2)x_5 + 2\Lambda_1 x_4 \quad (\text{A1e})$$

$$\partial_t x_6 = -2\Gamma \frac{x_8 x_6}{x_2} + \Lambda_1 x_5 - 2(\Lambda_2 + 1)x_6 \quad (\text{A1f})$$

$$\partial_t x_7 = \Gamma \frac{x_5 x_8}{x_2} + 2 \frac{x_3}{x_1 + x_2 + x_3} - (\Lambda_1 + 2 + W)x_7 + \Lambda_2 x_8 \quad (\text{A1g})$$

$$\partial_t x_8 = -\Gamma \left(\frac{x_8^2}{x_2} + 2\sigma^{-1} x_8 \right) + 2\Gamma \frac{x_6 x_8}{x_2} - (\Lambda_2 + 2)x_8 + (\Lambda_1 + W)x_7 \quad (\text{A1h})$$

$$\partial_t x_9 = \Gamma \left(\frac{x_8^2}{x_2} + 2\sigma^{-1} x_8 \right) - 2x_9. \quad (\text{A1i})$$

At steady state, the left hand side of the above equations is zero. We proceed in our derivation by dividing all equations in the steady state by x_2 and introducing a new variable $z_i \equiv x_i/x_2$, obtaining the following system of equations:

$$0 = 1/x_2 - \Lambda_1 z_1 + \Lambda_2 - z_1 \quad (\text{A2a})$$

$$0 = \Lambda_1 z_1 - \Lambda_2 - \Gamma z_8 - 1 \quad (\text{A2b})$$

$$0 = \Gamma z_8 - z_3 \quad (\text{A2c})$$

$$0 = \Lambda_2 z_5 + 2z_1 - 2(\Lambda_1 + 1)z_4 \quad (\text{A2d})$$

$$0 = 2 - \Gamma z_5 z_8 + 2\Lambda_2 z_6 - (\Lambda_1 + \Lambda_2 + 2)z_5 + 2\Lambda_1 z_4 \quad (\text{A2e})$$

$$0 = -2\Gamma z_8 z_6 + \Lambda_1 z_5 - 2(\Lambda_2 + 1)z_6 \quad (\text{A2f})$$

$$0 = \Gamma z_5 z_8 + 2z_3 - (\Lambda_1 + 2 + W)z_7 + \Lambda_2 z_8 \quad (\text{A2g})$$

$$0 = -\Gamma (z_8^2 + 2\sigma^{-1} z_8) + 2\Gamma z_6 z_8 - (\Lambda_2 + 2)z_8 + (\Lambda_1 + W)z_7 \quad (\text{A2h})$$

$$0 = \Gamma (z_8^2 + 2\sigma^{-1} z_8) - 2z_9. \quad (\text{A2i})$$

We have used the fact that in the steady state $x_1 + x_2 + x_3 = 1$, as can be shown by adding together the Eq.s (1a)-(1c). In the rest of the derivation we will find a closed equation for z_8 and express the other z_i 's in terms of z_8 .

We can immediately express z_1 , z_3 , and z_9 in terms of z_8 , by solving Eqs. (A2b), (A2c) and (A2i)

correspondingly:

$$z_1 = \Lambda_1^{-1}(1 + \Lambda_2 + \Gamma z_8) \quad (\text{A3})$$

$$z_3 = \Gamma z_8 \quad (\text{A4})$$

$$z_9 = (\Gamma/2)(z_8^2 + \sigma^{-1} z_8). \quad (\text{A5})$$

We substitute Eq. (A3) into Eq. (A2d), and Eq. (A4) into Eq. (A2g). The resulting two equations, together with Eqs. (A2e), (A2f) and (A2h), form a closed system of five equations with five unknowns z_4 - z_8 .

We solve the Eq. (A2f) for z_5 in terms of z_6 and z_8

$$z_5 = 2\Lambda_1^{-1}(1 + \Lambda_2 + \Gamma z_8)z_6, \quad (\text{A6})$$

and substitute the above result into Eq. (A2d) and (A2g), to solve for z_4 and z_7 in terms of z_6 and z_8 as follows:

$$z_4 = [(\Lambda_1 + 1)\Lambda_1]^{-1}[1 + \Lambda_2 + \Gamma z_8][1 + \Lambda_2 z_6] \quad (\text{A7})$$

$$z_7 = [\Gamma\Lambda_1^{-1}(2\Gamma z_8 + 2(\Lambda_2 + 1))z_6 + 2\Gamma + \Lambda_2] \times (\Lambda_1 + 2 + W)^{-1} z_8. \quad (\text{A8})$$

Substituting the expressions for z_4 and z_5 from Eq. (A6) and (A7) into Eq. (A2e), and solving for z_6 we obtain

$$z_6 = \frac{\Lambda_1}{\Gamma(\Lambda_1 + 1)z_8 + (\Lambda_1 + \Lambda_2 + 1)}, \quad (\text{A9})$$

Finally, substituting results of Eq.s (A9) and (A8) into Eq. (A2h) we obtain an equation for z_8 in a closed form:

$$\frac{[(a_1\Gamma)z_8^2 + (a_2\Gamma + a_3)z_8 + (a_4\Gamma^{-1} + a_5)]z_8}{[\Gamma(\Lambda_1 + 1)z_8 + (\Lambda_1 + \Lambda_2 + 1)]} = 0 \quad (\text{A10})$$

where

$$a_1 \equiv (\Lambda_1 + 1)(\Lambda_1 + W + 2) \quad (\text{A11})$$

$$a_2 \equiv 2\sigma^{-1}(\Lambda_1 + 1)(\Lambda_1 + W + 2) - 2(\Lambda_1 + 2)(W + \Lambda_1) \quad (\text{A12})$$

$$a_3 \equiv 3(\Lambda_1 + 1)(\Lambda_1 + W + 2 + \Lambda_2) + \Lambda_2(W + 1) \quad (\text{A13})$$

$$a_4 \equiv 2(\Lambda_1 + \Lambda_2 + 1)(\Lambda_1 + W + 2 + \Lambda_2) \quad (\text{A14})$$

$$a_5 \equiv (\Lambda_1 + \Lambda_2 + 1)[2(\sigma^{-1} - 2)(W + \Lambda_1) + 4(\sigma^{-1} - \Lambda_1)]. \quad (\text{A15})$$

Note that the physically relevant solutions are positive, and, therefore, finding a nontrivial solution of z_8 is a simple matter of solving a quadratic equation:

$$(a_1\Gamma)z_8^2 + (a_2\Gamma + a_3)z_8 + (a_4\Gamma^{-1} + a_5) = 0. \quad (\text{A16})$$

Solving Eq. (A2a) for x_2 , we can now express x_2 in terms of the newly found z_8 :

$$x_2 = \Lambda_1[(\Lambda_1 + 1)\Gamma z_8 + (\Lambda_1 + \Lambda_2 + 1)]^{-1}. \quad (\text{A17})$$

The rest of the original variables can be found using $x_i = x_2 z_i$. Thus, for example, x_3 is

$$x_3 = x_2 z_3 = \Gamma \Lambda_1 z_8 [(1 + \Lambda_1)\Gamma z_8 + (\Lambda_1 + \Lambda_2 + 1)]^{-1}. \quad (\text{A18})$$

Appendix B: Extremum of the mean degree in R-subnetwork

In steady state, the mean degree of the nodes within a R-subnetwork is found by taking a ratio of twice the number of RR-links to the number of R-nodes in the subnetwork:

$$\langle k \rangle = \frac{2\mathcal{N}_{\text{RR}}}{\mathcal{N}_{\text{R}}} = \frac{\mathcal{N}_{\text{RS}}}{\mathcal{N}_{\text{S}}} + 1 = \frac{\sigma}{2} z_8 + 1. \quad (\text{B1})$$

where the values of \mathcal{N}_{RR} and \mathcal{N}_{R} are obtained by solving Eqs. (1c) and (2f) in steady state. In this appendix we determine the value of Γ , Γ_m , that for

a given rewiring rate will maximize the degree in the resulting R-subnetwork. We do this by maximizing z_8 .

Differentiating Eq. (A16) with respect to Γ and evaluating the resulting equation at Γ_m , the value where extremum is attained, we obtain

$$a_1(z_8)_m^2 + a_2(z_8)_m - \Gamma_m^{-2} a_4 = 0. \quad (\text{B2})$$

Note that the derivative of z_8 with respect to Γ evaluated at Γ_m is equal to zero by definition, and the a_i are independent of Γ . Multiplying the above equation by Γ and subtracting it from Eq. (A16) evaluated at Γ_m allows us to solve for $(z_8)_m$:

$$(z_8)_m = -\frac{2a_4 + \Gamma a_5}{\Gamma a_3}, \quad (\text{B3})$$

Substituting the value of $(z_8)_m$ into Eq. (B2) and solving for Γ_m we obtain

$$\Gamma_m = [a_2 a_3 a_4 - 2a_1 a_4 a_5 + (a_2^2 a_3^2 a_4^2 + a_1 a_5^2 a_4 a_3^2 - a_2 a_3^3 a_5 a_4)^{1/2}] / [a_5(a_1 a_5 - a_3 a_2)], \quad (\text{B4})$$

the location of the maximum for the given rewiring rate.

-
- [1] I. J. Benczik, S. Z. Benczik, B. Schmittmann, and R. K. P. Zia, *EPL (Europhysics Letters)* **82**, 48006 (2008).
- [2] I. Benczik, S. Benczik, B. Schmittmann, and R. Zia, *Physical Review E* **79**, 046104 (2009).
- [3] B. Schmittmann and A. Mukhopadhyay, *Phys Rev E Stat Nonlin Soft Matter Phys* **82**, 066104 (2010).
- [4] P. Holme and M. E. J. Newman, *Physical Review E* **74**, 056108 (2006).
- [5] F. Meyer and A. Ultsch, in *Advances In Data Analysis, Data Handling And Business Intelligence*, German-Classification-Society (German-Classification-Society, 2010), pp. 419–427.
- [6] J. Bendor, B. A. Huberman, and F. Wu, *Journal Of Economic Behavior & Organization* **72**, 290 (2009).
- [7] M. A. Janssen and W. Jager, *Journal Of Economic Psychology* **22**, 745 (2001).
- [8] E. Abrahamson, *Scandinavian Journal Of Management* **25**, 235 (2009).
- [9] C. Grueter and F. Ratnieks, *Animal Behaviour* **81**, 949 (2011).
- [10] B. Benedict, *SIAM News* **40** (2007).
- [11] C. Kuhlman, V. Kumar, M. Marathe, S. Ravi, and D. Rosenkrantz, in *Machine Learning and Knowledge Discovery in Databases. European Conference, ECML PKDD 2010. Proceedings (ECML, 2010)*.
- [12] A. Gutfraind, *Terrorism as a mathematical problem*, *SIAM News* (2009).
- [13] A. Gutfraind, *Studies in Conflict and Terrorism* **32**, 45 (2009).
- [14] M. Johnson, N.F.and Spagat and O. e. a. Restrepo, J.A.and Becerra (2005), <http://arxiv.org/abs/physics/0506213>.
- [15] N. Johnson, S. Carran, J. Botner, K. Fontaine, N. Laxague, P. Nuetzel, J. Turnley, and B. Tivnan, *SCIENCE* **333**, 81 (2011), ISSN 0036-8075.
- [16] J. P. Caulkins, D. Grass, D. Feichtinger, and . Tragler, *Comp. Oper. Res.* **36** (2008).
- [17] L. B. Butler, *Tech. Rep. OMB No. 074-0188, SAMS Monograph, Fort Leavenworth, KS 66027-2134* (2011), contains many good references for recruitment, both stochastic and deterministic.
- [18] R. Lindelauf, P. Borm, and H. Hamers, *Social Networks* **31**, 126 (2009).
- [19] J. D. Farley, *Studies in Conflict and Terrorism* **26**, 399 (2003).
- [20] H. Bar-Isaac and M. Baccara, *Working Papers 06-07*, New York University, Leonard N.

- Stern School of Business, Department of Economics (2006), URL <http://ideas.repec.org/p/ste/nystbu/06-07.html>.
- [21] F. Udvardi, G. Leitmann, and L. Lambertini, *Discrete Dynamics in Nature and Society* **2006**, 85653 (2006).
- [22] A. Cherif, H. Yoshioka, W. Ni, and P. Bose (2009), arXiv/0910.5272.
- [23] K. Bentson, Master's thesis, Air Force Institute of Technology (2006).
- [24] T. Gross, C. J. D. D'Lima, and B. Blasius, *Phys Rev Lett* **96**, 208701 (2006).
- [25] L. Shaw and I. Schwartz, *Physical Review E* **77**, 066101 (2008).
- [26] D. Gillespie, *Journal of Computational Physics* **22**, 403 (1976).
- [27] M. J. Keeling, D. A. Rand, and A. J. Morris, *Proc Biol Sci* **264**, 1149 (1997), URL <http://dx.doi.org/10.1098/rspb.1997.0159>.
- [28] T. Gross and B. Blasius, *J R Soc Interface* **5**, 259 (2008), URL <http://dx.doi.org/10.1098/rsif.2007.1229>.
- [29] L. B. Shaw and I. B. Schwartz, *Phys Rev E Stat Nonlin Soft Matter Phys* **77**, 066101 (2008).